Analysis of Flocculation Activity of Microparticle Solution of Salty Protein from Whey of Oviparous Animals

Li, Fengzhen

College of Bioengineering, Hunan Polytechnic of Environment and Biology, Hengyang, 421005, P.R. CHINA

Huang, Xiaobo*+

Department of Environmental Science, Changsha Environmental Protection College, Changsha, 410004, P.R. CHINA

Mirzamani Bafghi, Seyed Mahmoud

Global inquiries and Social Theory Research Group, Ton Duc Thang University, Ho Chi Minh City, VIETNAM

ABSTRACT: *Because the traditional method does not consider the release rate of salty whey protein particles after adding flocculants, the error in the peak test of the flocculation activity of the ovarian animal whey protein particle solution is relatively high, which leads to the unreliable analysis of the flocculation activity. Therefore, a method is proposed. A new method for analyzing the flocculation activity of egg-shaped animal whey protein particle solution. According to the basic characteristics of whey protein, the basic structure of the flocculation model was reset to improve the purification effect of the whey protein particle solution in eggs. By calculating the loading rate and analyzing the effect of the flocculating carrier on the stability and release of individual particles, the release rate of salty whey protein particles after adding flocculants can be obtained. Combining the activity distribution with the propagation algebra, the flocculation activity analysis result is obtained. Experimental results show that this method can effectively reduce the error rate of the peak activity test, improve the reliability of the analysis of the flocculation activity of the ovarian animal whey protein particle solution, and has better stability and analysis effect than the traditional method.*

KEYWORDS: *Ovipara; Whey Salty Protein; Microparticle Solution; Flocculation Activity.*

INTRODUCTION

With the continuous innovation of technical means, the nutritional composition analysis of whey salty protein ovum animals is more and more in place. Various kinds of food developed by using whey salty protein of ovum

animals are more and more popular with public consumers. Therefore, in order to better analyze the microparticle solution of whey salty protein of ovum animals, the flocculating activity under the control of the flocculant is used to make diversified products. According to the characteristics of molecular adsorption, emulsification, and transport, the flocculation activity analysis results of protein microparticle solution were obtained [1–3]. However, in many experiments, the analysis results are not ideal. For example, there are studies using conventional bacterial isolation and purification methods to screen out 13 strains of flocculant-producing strains from sludge and soil and use the flocculants produced after 48 hours of cultivation. Analysis of the flocculation activity of the whey protein microparticle solution; some studies use polyacrylamide to add to the sample solution, by measuring the change of free Ca~(2+) concentration (or activity) during the flocculation process, to conduct research and determine other relationships, So as to realize the analysis of the flocculation activity of the whey salt protein particle solution. However, the analysis effect brought by the above analysis method is poor, and the release rate of salty whey protein particles after adding flocculant is not considered, which makes the peak test error of the flocculation activity of ovarian animal whey protein particle solution higher, which leads to the flocculation activity. The analysis result is unreliable, so a new method for analyzing the flocculation activity of whey salt protein particle solution is proposed. This method not only solves the problems of traditional methods but also provides reliable technical support for the development of flocculation activity analysis technology.

THEORETICAL SECTION
Analysis method of flocculation activity of whey salty protein microparticle solution of oviparous animals
Purification of albumin microparticle solution from the whey of oviparous animals

Egg white refers to the transparent gelatinous substance wrapped around the egg yolk. It is a typical colloidal solution with protein as the dispersion phase and water as the dispersion phase. It is divided into frenum, frenum membrane, inner thin protein, thick protein, and outer thin protein. Under the action of whey, these proteins produce salty proteins with a salt content of up to 7% ~ 12%.

See Table 1 for details.

It is known that under natural conditions, the reaction groups such as hydrophobic groups and hemifulaminic acid residues are located inside the molecule, and the attraction between protein molecules is mainly hydrophobic interaction and van der Waals force, which are not enough to overcome the repulsion between molecules, including electrostatic interaction, hydration, and dihydric force, so molecules generally exist in the form of monomers or small aggregates. Therefore, after heat treatment, the internal energy of the system increases, the degree of thermal movement of protein molecules increases, the vibration frequency and amplitude of some groups in the molecule increase, the spatial structure of protein changes, and the skin chain changes from curling to stretching, the static charge on the surface of the unfolded skin chain becomes thinner, and the attraction between particles becomes larger so that they are easy to approach each other and pass through the hydrophobic groups and Ryukyu formed intermolecular hydrophobic bonds and disulfide bonds, which resulted in a certain degree of aggregation between colloidal particles. If the protein concentration is smaller than the critical concentration of the gel, with the increase of the aggregation degree, the volume of the aggregate will increase, and the thermal resistance will increase. The increase of the surface charge and hydrophilic group will reduce the attraction between the aggregates and the rate of aggregation will slow down. Finally, a relatively stable system will be formed, most of which are soluble aggregates. Part of the higher degree of aggregation produced precipitation. Therefore, by changing the aggregation conditions, such as temperature, pH, ion concentration, protein concentration, etc., we can change the balance of repulsion and attraction in the protein system, thus forming different aggregation forms, such as fibrotic aggregation, granular aggregation, and amorphous aggregation. The aggregation of salty protein microparticles is a multi-level aggregation process, and temperature is the dynamic mode of salty protein aggregation. Under the action of whey, the salt protein after ultra-high temperature treatment mainly aggregates by disulfide bond, while the protein after ordinary high-temperature treatment aggregates by hydrophobic interaction, and the molecular conformation is more flexible.

Table 1: Types and properties of proteins.

Protein type	Content/%	Molecular weight/kDa	Isoelectric point	Denaturation temperature/°C	Disulfide bond	Free thiol number
Ovalbumin	54	45	4.5-4.9	75-84	1	4
Egg with albumin	12-13	77.7	6.0-6.1	61-65	15	-
Ovomucin	11	28	4.1	77	9	-
mucin	1.5-3.5	5500-8300	4.5-5.0	-	-	-
Lysozyme	3.4-3.5	14.3-14.6	10.7	69-77	5	-
Oocyte G2	1.0	47-49	4.9-5.5	92.5	-	-
Oocyte G3	1.0	49-50	4.8,5.8	-	-	-
Yolk protein	0.8	32-38	4.0	-	2	-
Ovoprotein	0.5	760-900	4.5-4.7	-	-	-
Antibiotic protein	0.05	55-68.3	10.0	-	1	-

pH mainly affects the static charge of protein molecules, and the charge of protein will affect the interaction between and within the molecules, resulting in the change of surface hydrophobicity and secondary structure of protein molecules. The ionic strength mainly controls the electrostatic interaction of protein particles in solution. A certain ionic strength can shield the surface charge of protein through electrostatic interaction, which makes hydrophobic groups easy to be exposed to and aggravates the aggregation of the protein. With the increase of ionic strength, excessive ions will increase the interaction between protein molecules and solvents, thus inhibiting protein aggregation. Whey concentration mainly controls the reaction speed of molecules, and increasing whey concentration will increase the chance of protein molecules colliding with each other. When whey concentration is greater than or equal to the critical concentration of gel, a wide range of cross-linking can be formed between protein aggregates, forming a highly ordered three-dimensional network structure that can maintain a large amount of moisture. In this process, the repulsion and attraction are in equilibrium.
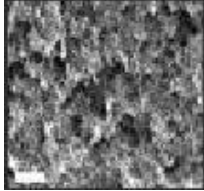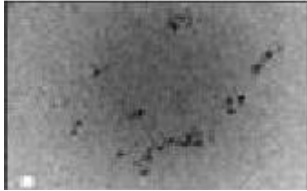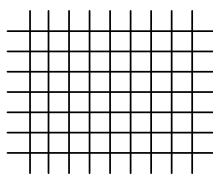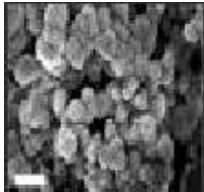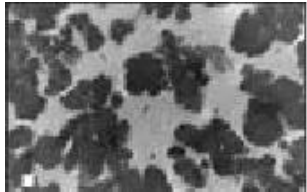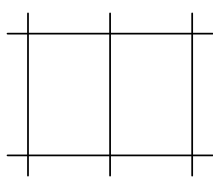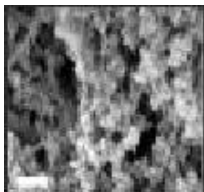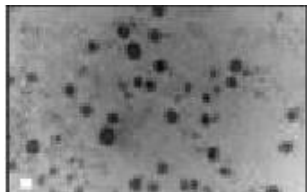
Almost all proteins are globulin, and the formation of globulin gel is a complex process, which generally involves many reactions, such as protein denaturation, dissociation, aggregation, and so on. Proteins from different gels with different textures function through different aggregation ways. Therefore, according to the above-mentioned factors, it is easy to form a fine linear gel when the pH value is far away from the isoelectric point
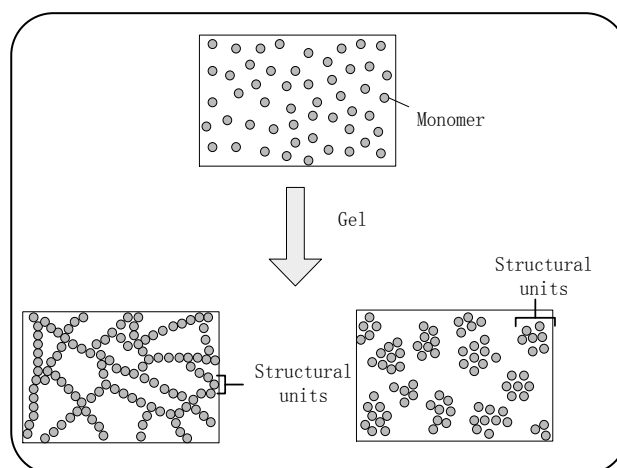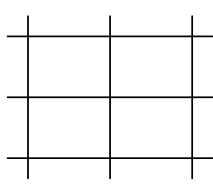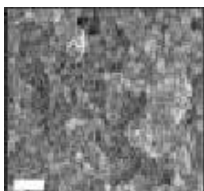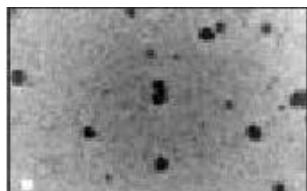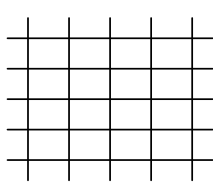

Fig. 1: Schematic diagram of linear gels and granular gels.

and the ionic strength is relatively low. When the pH value is near the isoelectric point or the ionic strength is high, it is easy to form a granular gel, as shown in Fig. 1.

In addition, there are two types of intermediate structures, i.e. linear structure and granular structure. Under different pH and ionic strength conditions, four different types of protein heat-induced gelatin were obtained. The protein microparticle solution was generally divided into four types: divisible gel, granular sponge gel, intermediate gel, and smooth rigid gel. The type of gel depends on the morphology, quantity, and organization of different aggregates. For particulate sponge-like gel obtained at pH 5, near isoelectric point and ionic strength, interspaced large spherical aggregates were observed in frozen TEM and SEM micrographs. On the contrary,

Table 2 Morphology, microstructure, and mesh of different gel types of proteins

Processing conditions	Form	Microstructure (SEM)	Microstructure (cryo-TEM)	Mesh diagram
pH 2/IS 0.05 M	Dividable gel			
pH 5/IS 1 M	Granular sponge gel			
pH 7/IS 0.05 M	Intermediate gel			
pH 9/IS 0.05 M	Smooth rigid gel			

segmented gels were obtained under conditions of pH 2, 7 and 9, and the intermediate gel and smooth rigid gel consisted of spherical aggregates and linear aggregates. According to the type of gel, the relative volume and organization mode of the two different aggregates are different. In the divisible gel, the number and size of spherical aggregates are the smallest and the linear aggregates are organized into a tight mesh. In smooth rigid gel, spherical aggregates are larger and more round, and linear aggregates are more compact. In the intermediate gel, the volume of spherical aggregates is the largest, and the gel tends to consist of linear branching aggregates which form different clusters. Therefore, the meshes size of intermediate gel is larger than that of divisible gel and smooth rigid gel. The data in Table 1 below are the basic information of whey protein microparticles of ovum animals in solution [4].

It is found that the water-holding rate of protein gel is related to the structure of aggregation. Large volumes and compact structures form a rough gel with less microstructure. At the same time, the gel formed by these larger aggregates has lower hardness. The water holding rate of gel with low hardness and low hardness is low, and the water is easier to seep from the gel under the applied force. Therefore, to control the aggregation morphology and aggregation mode of protein molecules and analyze the flocculation activity of microparticle protein solution, it is necessary to purify the protein [5].

Dissolve the extracted protein in distilled water, adjust the pH value to reach 8.5, and then place it in a centrifuge to remove the precipitate under the condition of 4000r/min for 10 min. Then the supernatant was adjusted after centrifugation so that the pH value of the supernatant reached 6, three times the volume of ethanol was added to it, and 30 min was precipitated. The precipitated protein was collected and washed with acetone two times, dried, and the chromatograph.

Table 3: Protein components after separation and purification.

Amino acid	Composition (g/100g)		
	I	II	III
Aspartic acid	2.46	0.35	2.53
Threonine	3.47	0.51	4.76
Serine	5.44	6.54	5.72
Glutamic acid	5.17	1.15	4.73
Glycine	3.10	2.87	2.56
Alanine	19.16	1.74	17.57
Tyrosine	7.43	4.44	4.93
Isoleucine	0.92	1.07	1.13
Leucine	2.04	0.00	3.16
Tyrosine	1.62	0.65	1.00
Phenylalanine	0.86	0.00	0.67
Lysine	37.36	1.62	39.24
Histidine	0.00	0.04	0.40
Arginine	2.42	73.46	1.92
Proline	8.54	5.56	9.64

Take about 30 mL CM Sepharose fast flow cation exchange chromatography packing into a 200 mL beaker, add distilled water of 5 times the volume of 0.22 μm filter membrane, wash it 3-5 times, to remove the ethanol attached to it, and then wash the packing for 2-3 times with a 50 mmol/L slow flushing solution of potassium dihydrogen phosphate sodium hydroxide (pH = 8.0), and then install the column. The column volume is about 30 mL, and then use 3-5 column bed volumes of 50 mmol/L potassium dihydrogen phosphate sodium hydroxide buffer solution with pH of 8.0 to balance the column. The wavelength of UV detector is 280 nm. After the baseline on the computer is stable, prepare the sample. The concentration of the sample solution is 10 mg/mL and the volume of each sample is 3 mL. after the sample is loaded, first use 50 mmol/L potassium dihydrogen phosphate sodium hydroxide buffer solution to elute 30 mL/min at the rate of 1.5 mL/min After that, a 50 mmol/L potassium dihydrogen phosphate sodium hydroxide solution containing 0 - 1.2 mol/L NaCl at pH8.0 was eluted with a gradient elution apparatus. The protein content in each tube was detected by Folin phenol method. The target protein was identified by sakakou reactions and SDS precipitation reactions. The protein components were collected and desalted in a dialysis bag with a molecular weight of 2000 Da. After concentration, the protein was freeze-dried and collected for bacteriostatic activity, flocculation activity detection, and amino acid composition analysis. The following Table 3 shows the components of purified ovum animal protein [6].

According to the data in the above table, calculate the surface hydrophobicity parameter of the protein, and determine the ion concentration in the purified protein microparticle solution according to the parameter. The following formula is the calculation expression of the hydrophobicity parameter:

$$\frac{1}{p} = \frac{1}{p_{max}} + \frac{u_d}{p_{max}} \cdot \frac{1}{N_0} \tag{1}$$

In the formula, p represents the fluorescence intensity of the sample; p_{max} represents the maximum relative fluorescence intensity when the probe concentration reaches saturation; u_d represents the apparent binding and dissociation constant of protein molecules and whey; N_0 represents the whey concentration, in μmol/L. Fig. 2 below is the schematic diagram of the ion concentration curve
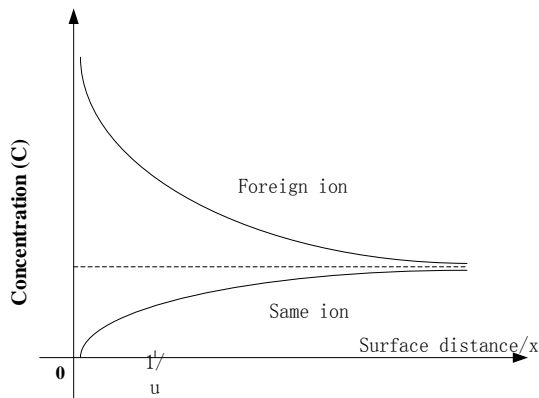
Fig. 2: Ion concentration distribution curve.

in the purified protein microparticle solution under the influence of surface hydrophobicity parameters [7].

It is known that inorganic flocculants can be divided into inorganic low salt and inorganic high polymer flocculants, and inorganic low molecular salt flocculants. The flocculation situation of the dispersion system can be summarized as follows: inorganic substances are ionized in solution, and heteroelectric ions with opposite electrical properties to charged particles are chemically adsorbed on the surface of particles, thus reducing the surface potential, reducing the repulsive potential energy between particles, and collision between particles will be easier; at the same time, if we continue to increase the concentration of electrolyte, it will make the charged property of particle surface opposite to the original one, and then the system will be stabilized again. The structural characteristics of the flocculation model of the inorganic flocculant are known. According to the purified solution ions, the model is improved to achieve a more accurate flocculation activity analysis. Fig. 3 is the schematic diagram of the improved model [8].

According to the improved flocculation model, the influence of the flocculation carrier on the stability and release of haploid microparticles was analyzed.

Obtain the effect of flocculation carrier on the stability and release of haploid microparticles

The protein was dispersed in a 20 mM phosphoric acid buffer (pH7.0) at a concentration of 0.5 wt.% and stirred magnetically for 1 h at 25℃. The conjugated linoleic acid was dissolved in anhydrous ethanol at different concentrations. 500 μL of conjugated linoleic acid

solutions of various concentrations were added to LP dispersion (9.5 mL). LP protein nanoparticles loaded with conjugated linoleic acid were prepared by ultrasonic treatment in an ice bath with 30% power for 5 min. In order to improve the stability of colloidal particles, nanoparticle dispersion loaded with conjugated linoleic acid was mixed with equal volume sodium caseinate solution, and the final concentration of sodium caseinate was 0-0.25wt.%, which was stirred at 200 rpm for 30 min. As a control, conjugated linoleic acid was embedded in sodium caseinate particles as a contrast. The solution of conjugated linoleic acid dissolved in anhydrous ethanol was dropped into 6wt.% sodium caseinate solution (9.5mL), so that the final concentration of conjugated linoleic acid was 1mg/mL, and then stirred for 30minx at 800 rpm on a magnetic stirrer. The preparation of conjugated linoleic acid-loaded LPP was realized [9].

The sample was diluted with 20 mM phosphate buffer (pH 7.0) to 1 mg/mL and then loaded into the sample tank for determination. All samples were tested 3 times at 25℃. The refractive index of the dispersed phase is 1.45 and that of the continuous phase is 1.331. The apparent hydrodynamic radius of the protein sample was analyzed by the method of "accumulation" in the software of the instrument and the Stokes-Einstein equation, and the particle size distribution and electric charge were measured.

The loading rate is the ratio between the mass of the entrapped conjugated linoleic acid and its total mass in the dispersed phase. Petroleum ether was used as an extractant to extract conjugated linoleic acid without load on the surface of the carrier. That is to say, at 60 ℃, 10 mL of sample is mixed with an equal volume of petroleum ether. Slowly shake the beaker for 10 minutes to extract the conjugated linoleic acid on the particle surface. After filtration, the filtrate is collected and evaporated to measure the content of conjugated linoleic acid on the surface of particles. The load rate is calculated as follows:

$$\mu = \frac{1}{p} \cdot \frac{x_{total} - x_1}{x_{total}} \times 100\% \tag{2}$$

In the formula, μ is the loading rate, unit is%; x_{total} is the total mass of conjugated linoleic acid; x_i is the mass of surface conjugated linoleic acid. According to the above formula, the load rate can be determined [10].

The morphology of colloidal particles was observed by transmission electron microscope. Add 2 μL of sample
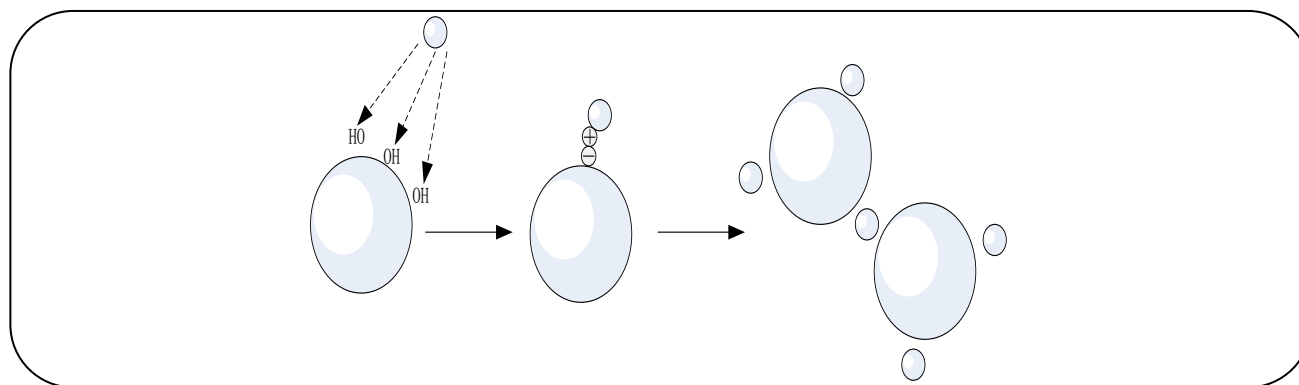
Fig. 3: Flocculation model of modified protein microparticle flocculant

the carbon-plated copper grid carefully absorbs the excess sample liquid with filter paper and dries at room temperature for 72h. Then the back of the sample was stained with phosphotungstic acid, dried after 60 s, and placed on the sample table for observation to determine the carrier microstructure characterization.

The resolution of 4 cm^{-1} is in the range of 4000 cm^{-1} and 400 cm^{-1} wave numbers, and the average value is obtained by scanning 64 times. In the preparation of the powder sample, add 1 mg sample to 100 mg KBr and grind to prepare KBr tablet. In the preparation of the liquid sample, evenly smear a thin layer of conjugated linoleic acid on KBr tablet. Set the scanning rate of cuka ray (40kV, 100 mA) to 5°/min. The oxygen consumption of conjugated linoleic acid in different carriers was determined by gas chromatography. 10 mL protein sample containing 1 mg/mL was placed in a serum bottle (20 mL) and sealed, and placed at 50℃ for 84h. The same amount of undivided protein solution was used in the control group. The headspace oxygen content was analyzed by GC. The oxidation stability of conjugated linoleic acid in protein nanoparticles was analyzed by measuring the oxygen consumption in the headspace and the peroxide value stored at 50℃ at different times. Fig. 4 below shows the headspace oxygen consumption of conjugated linoleic acid in different carriers.

As can be seen from the above figure, the oxygen concentration of all samples decreases with the increase in storage time. The consumption of oxygen is related to the oxidation of conjugated linoleic acid to form fatty oxide. When stored at 50℃ for 84h, the oxygen consumption of conjugated linoleic acid dissolved in ethanol is the most. However, the oxygen consumption of conjugated linoleic acid loaded in sodium caseinate is relatively small, and
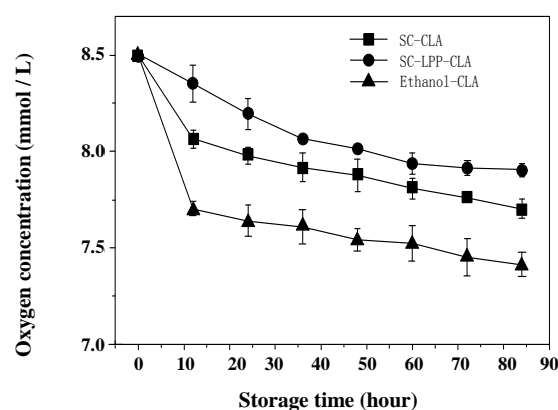

Fig. 4: Headspace oxygen consumption of conjugated linoleic acid in different carriers.

the oxygen consumption of conjugated linoleic acid loaded in protein nanoparticles are the least. This shows that the above two carrier loading of conjugated linoleic acid can increase its oxidation stability. Some studies have shown that proteins have an antioxidant capacity, which may partly explain the above phenomenon. However, the oxidation rate of conjugated linoleic acid loaded by sodium caseinate and protein nanoparticles is different, indicating that protein nanoparticles have a better protective effect on the oxidation of conjugated linoleic acid [11]. The hydrogen peroxide content of the sample containing 1 mg/mL of conjugated linoleic acid was determined during storage at 50℃, as shown in Fig. 5 below.

It can be seen from the figure that in the first 5 days, the concentration of hydrogen peroxide in all samples was relatively stable, and after 5 days, the concentration of hydrogen peroxide increased due to the oxidation of conjugated linoleic acid. The content of hydrogen peroxide in ethanol conjugated linoleic acid and sodium caseinate
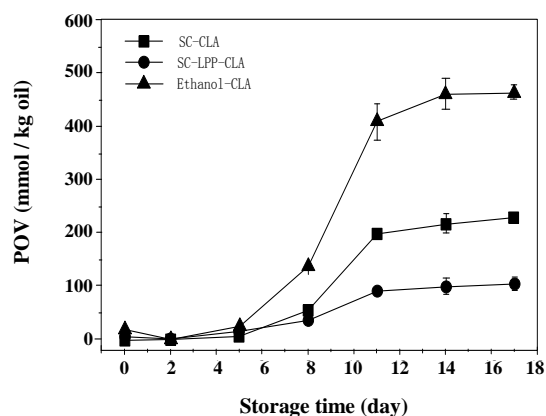
Fig. 5: Headspace oxygen concentration changes of conjugated linoleic acid during storage.

Fig. 6: Cumulative release of conjugated linoleic acid.

conjugated linoleic acid increased rapidly from the 5th to the 11th day and then increased slowly. However, the hydrogen peroxide content of conjugated linoleic acid is loaded in protein nanoparticles. Keeping this low growth rate, the hydrogen peroxide produced the least, which shows that soybean lipophilic protein nanoparticles can provide the best oxidation stability for conjugated linoleic acid in all samples [12].

The sustained-release characteristics of the carrier can protect the bioactive components, prevent premature digestion and avoid excessive exposure to the environment, so as to promote their effective absorption. The release characteristics of conjugated linoleic acid loaded on different carriers were analyzed. Fig. 6 shows the cumulative release of conjugated linoleic acid in vitro digestion at different digestion times.

The first 120 min indicates the beginning of simulated flocculation, and the next 210 min indicates the formation of simulated flocculation. For sodium caseinate granules, the release rate of conjugated linoleic acid was very fast in the first 60 minutes, about 50%, and further increased to 69% in the next 270 minutes. For protein-conjugated linoleic acid particles, the release rate of conjugated linoleic acid remained unchanged in the whole process. The total final release of conjugated linoleic acid in protein conjugated linoleic acid granules was about 30% in 330 min. The results show that the delivery system of conjugated linoleic acid of protein nanoparticles can slow down the release of conjugated linoleic acid. According to the above analysis, when the hydrophobic components are loaded, the sodium caseinate particles show a cluster
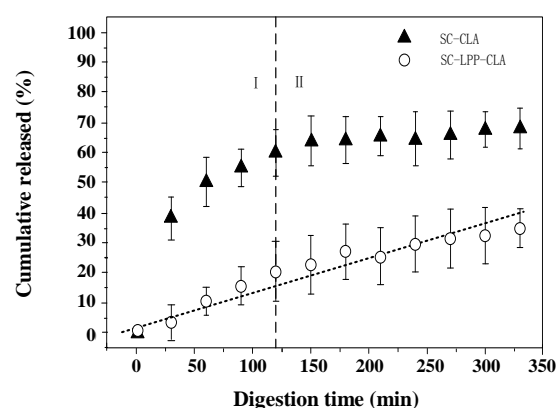
core-shell structure, in which the hydrophobic substances exist in the core, and the sodium caseinate aggregates around to form a shell. Therefore, with the degradation and collapse of the core-shell structure in the process of enzyme digestion, the conjugated linoleic acid loaded in the sodium caseinate particles is released directly, resulting in rapid release in the initial stage. The lower release rate in the later stage may be related to the hydrolytic release of proteins binding to conjugated linoleic acid. Although protein nanoparticles can also be hydrolyzed in the digestion process, the carrier structure is gradually hydrolyzed layer by layer and will not collapse in a short time. However, the release of conjugated linoleic acid depends on the gradual hydrolysis of protein, so it can avoid a large amount of release in a short time, and its release process almost follows the first-order kinetics. The release rate of conjugated linoleic acid was effectively controlled by the complete combination of conjugated linoleic acid and carrier. It can be seen that as the carrier of conjugated linoleic acid, protein nanoparticles can not only achieve a high loading rate and provide good oxidation protection, but also achieve slow release [13].

Determination of flocculation activity of microparticle solution

Make a series of dilutions for the flocculation sample, and then take a certain amount of diluent to inoculate it into the culture dish so that it is evenly distributed in the protein solution culture medium on the plate. After constant temperature culture at 30℃, a single cell grows and propagates to form a colony, and then counts the number

of colonies and converts the number of bacteria in the sample. Because the sample to be tested is not easy to completely disperse into a single cell, a single colony may also grow from two, three, or more cells in the sample. Therefore, the results of plate colony count are often low. In order to clearly explain the results of plate counting, colony-forming units have been used instead of absolute colony numbers to express the live bacteria content of samples. The biggest advantage of this counting method is that it can obtain information on live bacteria.

The fermentation medium without inoculation was used as blank control, and the wavelength of 600 nm was selected for turbidimetric determination. The culture medium with high cell density was diluted with a fermentation medium, and the absorbance was within 0.1 to 1.0. Using intelligent coagulation test mixer and coagulation test mixer to determine the flocculation effect of flocculant on protein microparticle solution. Add a certain amount of bioflocculant culture solution and solution sample in the order of 1000mL of solution sample to be tested, and then adjust the pH value of the sample to about 7.2 with 2mol/L NaOH solution or 2mol/L HC1 solution. At the same time, the sample solution without any flocculant under the same conditions was used as the blank control. After the completion of mixing with the six-unit coagulation agitator, the static precipitation is carried out for 20min. In the water temperature measurement, the hydraulic condition is two-stage mixing, the first stage mixing speed is 160r/min, mixing time is 40s; the second stage mixing speed is 40 r/min, mixing time is 280s. The transmittance of supernatant was measured at 550nm with 721 spectrophotometer [14]. The flocculation effect is characterized by flocculation efficiency. The formula is as follows:

$$q(\%) = \frac{U - V}{\mu V} \times 100\%$$ (3)

In the formula: *U* represents the turbidity (light transmittance) of the supernatant of the blank solution sample, and *V* represents the turbidity (light transmittance) of the supernatant of the solution sample to be tested. Flocculation rate *q* refers to the removal rate of suspended solids in solution before and after adding flocculant, namely flocculation rate. According to the results of the above formula, the distribution state of the flocculating active components is determined. First of all, a certain amount of bioflocculant fermentation liquid will be

centrifuged, combined with the observation of an optical microscope and the measurement of the flocculation rate effect, to investigate the influence of centrifugal speed and centrifugal time on the separation effect of bacteria and their secretions, and determine the centrifugal method as follows: the fermentation liquid is centrifuged at 12000r/min, 4°C for 20min. Then take 10mL of bioflocculant fermentation liquid, separate it by centrifugation, collect the supernatant, and dilute it to 30mL for standby. Take a certain amount of fermentation liquid and three times the volume of supernatant, and test the flocculation effect by coagulation cupping test, that is to say, investigate the flocculation activity of fermentation liquid and bacterial secretion respectively, and characterize it by the distribution of flocculation activity *s*. The following formula is the calculation result:

$$s = \frac{q_i}{q_j} \times 100$$ (4)

In the formula, q_i is the flocculation rate of the supernatant with the concentration of fermentation liquid, and q_j is the flocculation rate of the supernatant with the centrifugation parameter of fermentation liquid as *j*. Flocculation activity distribution *S* is essentially the proportion of the secreted active substances in the overall flocculation capacity of the bioflocculant [15]. According to the above calculation results, the growth curve of flocculating bacteria was determined. According to the growth rate constant, the typical growth curve can be roughly divided into four periods: delay period, index period, stability period, and decay period. In the exponential growth period, three parameters are the most important. The calculation formula of these three parameters is:

$$N = \frac{\lg \sigma_2 - \lg \sigma_1}{s \lg 2} = 3.322 \times (\lg \sigma_2 - \lg \sigma_1)$$ (5)

Where: σ_1 and σ_2 represent the number of cells before and after flocculation respectively; *N* represents the generation algebra. According to the calculation results, the expression of the growth rate constant is obtained.

$$K = \frac{N}{D_2 - D_1} = \frac{3.322 \times (\lg \sigma_2 - \lg \sigma_1)}{D_2 - D_1}$$ (6)

Where: D_1 and D_2 represent the change cycle function before and after flocculation respectively. Combining

formula (5) and formula (6), the objective function lne is introduced to obtain the generation parameter

$$G = \frac{1}{K} \ln e = \frac{D_2 - D_1}{3.322 \times (\lg \sigma_2 - \lg \sigma_1)} \ln e \quad (7)$$

In order to ensure that the error of the measurement results can be minimized, the plate counting method, turbidimetric method, and dry weight method are used to test the flocculation activity curve of protein microparticle solution, as shown in Fig. 7-1, 7-2 and 7-3 below [16].

According to the above three groups of test results, there is basically no lag period after the flocculating bacteria are connected to the liquid culture medium, which is due to the reason that the age and inoculation amount of the selected bacteria are more appropriate. In 0-15h, the growth of flocculating bacteria is in the exponential growth period, the absorbance, colony number, and dry weight of the fermentation liquid are obviously increasing, the nutrient substance in the culture medium is relatively sufficient, the cell growth is unlimited, and the cell concentration increases exponentially with time; in 15-27h, the growth of flocculating bacteria enters the stable period, and the absorbance of the fermentation liquid is slowly increasing, because of a large number of cells after 27h, the growth of flocculating bacteria enters the decay period, and the cells in the culture medium begin to die, as shown in Fig. 7-1, the concentration of living cells begins to decline, but the absorbance and dry weight of the fermentation liquid gradually increase, as shown in Fig. 7-2 and Fig. 7-2 Fig. 7-3. It should be pointed out that in Fig. 7-2, after 33 hours, the absorbance no longer changes, and the absorbance is saturated. This is due to the fact that the number of living bacteria and dead bacteria measured by the dry weight method in the test, so the dry weight in the decay period is on the rise; Turbidimetric method is used to measure the turbidity of fermentation broth, but it will cause the increase of turbidity after the death of bacteria, which will lead to the gradual increase of absorbance of fermentation broth, so the absorbance is still increasing in the decay period; plate colony count method is used to measure the number of living bacteria in the fermentation broth, so the trend it shows is the real growth trend of bacteria. However, because the turbidimetric method is simple and rapid, and the results measured in the early stage of fermentation are little affected by external factors, when the fermentation time of
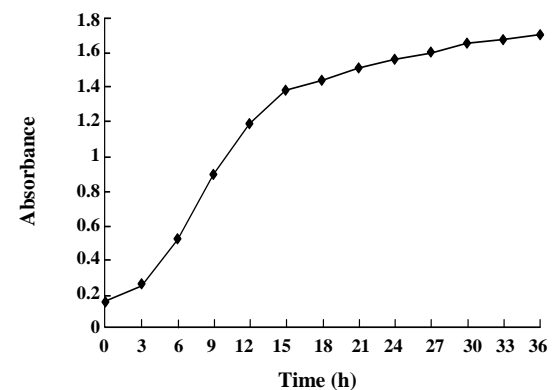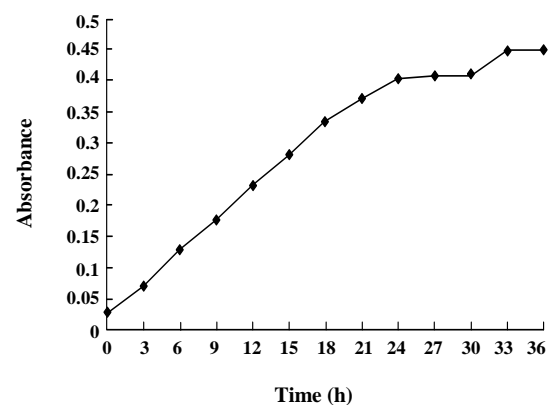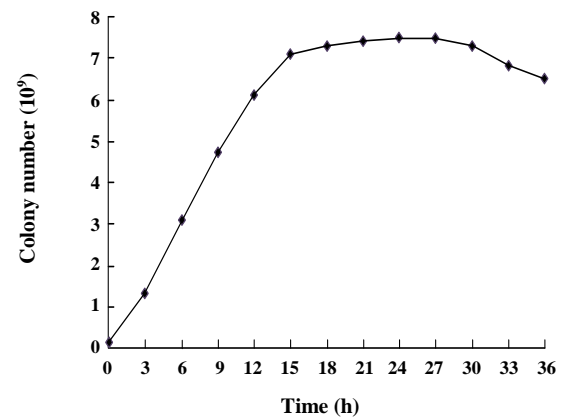

Fig. 7: 1) Plate counting method measurement results, 2) Bacteria determination results, 3) Dry weight measurement results.

flocculating bacteria is within 0-36h, the turbidimetric method is still used to reflect the growing trend of bacteria, and the dry weight method is used to reflect the change of bacteria volume. The actual values of three parameters of flocculating bacteria can be obtained by substituting the number of logarithmic long-term colonies in Fig. 7-1
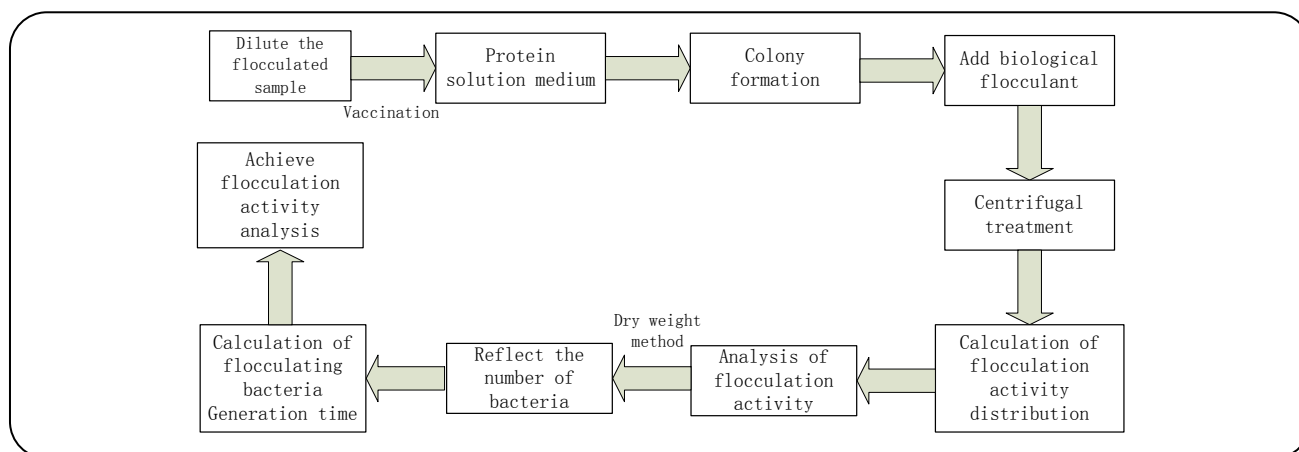
Fig. 8: Process steps for determination of flocculation activity of particle solution.
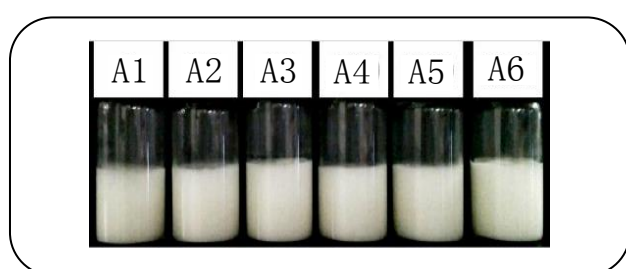

Fig. 9 Experimental test objects

into equations (5-7) respectively. According to this value, the generation time of the flocculent bacteria was calculated under the condition of 30 ℃ temperature, rotating speed of the shaking table of 150 rpm, and inoculation amount of 10%. So far, the flocculent activity analysis method of whey salty protein microparticle solution of Oozoan was realized [17].

Based on the above analysis, the process steps for the determination of the flocculation activity of the particle solution as shown in Fig. 8 are obtained.

EXPERIMENTAL SECTION

In order to further verify the superior application performance of this method, a comparative experiment was carried out to test the proposed analysis method and the traditional analysis method, and the reliability of the flocculation activity was analyzed at the same time. First, set up the experimental test platform, and select and configure the experimental test objects. To ensure the scientificity and rigor of the experimental results, two test objects are configured for each type, as shown in Fig. 9.

The A1 and A2 shown in the figure refer to the flocculation activity analysis object of the analysis method

proposed in this paper; A3 and A4 refer to the flocculation activity analysis object of the traditional analysis method; A5 and A6 refer to the spare experimental object. Using the test object shown in Fig. 9, the analysis method proposed in this paper was set as the experimental group, and the traditional analysis method was set as the control group. The flocculation activity analysis of the oviparous whey protein microparticle solution was performed to verify the reliability of the analysis method. , The peak activity test was performed on the two groups of test subjects, and the comparison chart of the test results is shown in Fig. 10.

According to the above two groups of test results, under the same test time, the two groups of data in the experimental group reached peak activity in the 8th to 10th hours (As shown in Fig. 10-1). In the same experimental subjects, the two groups of data in the control group reached the highest activity value at the 5th and 8th hours (As shown in Fig. 10-2). Analyze Fig. 10-1 and Fig. 10-2 at the same time, and get the result: Although the test error cannot be avoided, under the same experimental test environment, it can be clearly seen that the peak activity value error obtained by the analysis method proposed in this paper is small. The activity values of the two groups of data in Fig. 10-1 are similar; while the objects tested by the traditional analysis method have great errors in more than 3 hours. The activity values of the two groups of data in Fig. 10-2 the degree value has a large difference. In summary, the analysis method proposed in this paper has fewer errors in peak activity tests and has high analytical reliability. Therefore, the method proposed in this paper is due to traditional analysis methods.
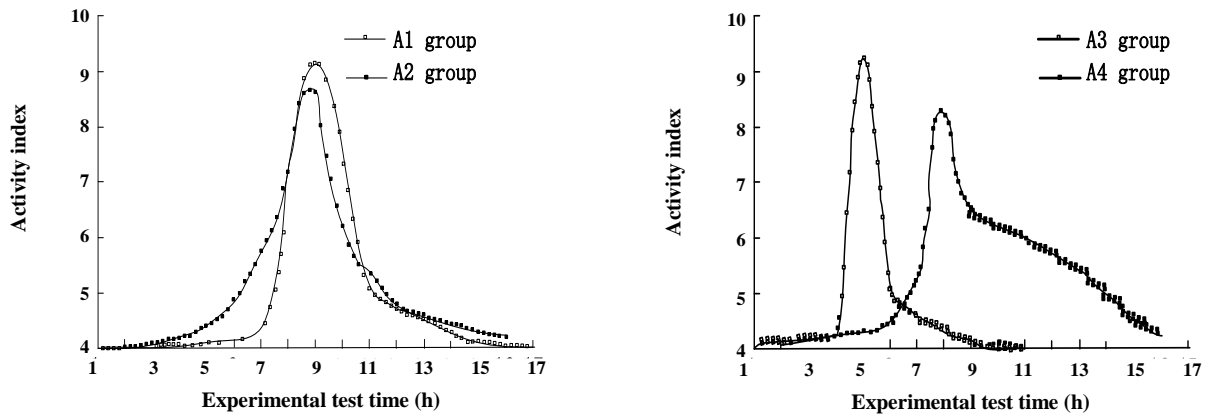
Fig. 10: 1) Test results of the experimental group, 2) Control test results.

CONCLUSIONS

In this paper, the flocculation model is reconstructed to purify the whey protein particle solution, and the influence of the flocculation carrier on the stability and release of individual particles is analyzed to obtain the release rate of salty whey protein particles after adding flocculants, thereby completing the flocculation A new method of activity analysis, which reduces the error of the peak activity value of the flocculation of the microparticle solution and improves the reliability of the analysis of the flocculation activity of the whey salty protein microparticle solution. The results obtained through experimental tests verify that the analysis method proposed in this paper is more practical for the analysis of the flocculation activity of egg-laying animal whey salty protein microparticle solution, which meets the requirements of experimental testing and detection. However, the analysis method proposed this paper still has certain problems. For example, the influence of flocculating bacteria metabolism on the analysis of flocculation activity is not considered in the research, which needs further analysis and discussion in future research.

REFERENCES

[1] Nam Y-J., Cho C-H., Kim L., Lee H-J., Association of G-protein β3 Subunit C825T Polymorphism with Seasonal Variations in Mood and Behavior, *Psychiatry Investig*, **15**: 200 (2018).

[2] Vedadghavami A., Minoei F., Hosseini S.S., Practical Techniques for Improving the Performance of Polymeric Membranes and Processes for Protein Separation and Purification, *Iran. J. Chem. Chem. Eng. (IJCCE),* **37**: 1–23 (2018).

[3] Majidi B., Fathi Najafi M., Saeedyan S., Expression and Purification of Brucella Spp Lumazine Synthase Decameric Carrier in Fusion to Extracellular Domain of Influenza M2E Protein, *Iran. J. Chem. Chem. Eng. (IJCCE),* **40(6)**: 2061-2068 (2021).

[4] Kalin N.H., Corticotropin-Releasing Hormone Binding Protein: Stress, Psychopathology, and Antidepressant Treatment Response, *Psychiatry,* **175(3)**: 204-206 (2018).

[5] Hur N.W., Kim H.C., Waite L., Youm Y., Is the Relationship Between Depression and C Reactive Protein Level Moderated by Social Support in Elderly?-Korean Social Life, Health, and Aging Project (KSHAP), *Psychiatry Investig*, **15(1)**: 24 (2018).

[6] Hauptmann A., Podgoršek K., Kuzman D., Srčič S., Hoelzl G., Loerting T., Impact of Buffer, Protein Concentration and Sucrose Addition on the Aggregation and Particle Formation During Freezing and Thawing, *Pharm. Res*., **35**:101 (2018).

[7] Sun Y., Ren T., Deng Z., Yang Y., Zhong S., Molecularly Imprinted Polymers Fabricated Using Janus Particle-Stabilized Pickering Emulsions and Charged Monomer Polymerization, *New J. Chem.,* **42**:7355–7363 (2018).

[8] Lourenc□o A., Arnold J., Cayre O.J., Rasteiro M.G., Flocculation Treatment of an Industrial Effluent: Performance Assessment by Laser Diffraction Spectroscopy, *Ind. Eng. Chem. Res.*, **57**:2628–2637 (2018).

[9] Kutzli I., Gibis M., Baier S.K., Weiss J., Fabrication and Characterization of Food- Grade Fibers from Mixtures of Maltodextrin and Whey Protein Isolate Using Needleless Electrospinning, *J. Appl. Polym. Sci.,* **135**: 46328 (2018).

[10] Song Z., Niu C., Wu H., Wei J., Zhang Y., Yue T., Transcriptomic Analysis of the Molecular Mechanisms Underlying the Antibacterial Activity of IONPs@ pDA-Nisin Composites toward Alicyclobacillus Acidoterrestris, *ACS Appl Mater Interfaces*, **11**: 21874–21886 (2019).

[11] Welker A., Cronenberg T., Zöllner R., Meel C., Siewering K., Bender N., Hennes M., Oldewurtel E.R., Maier B., Molecular Motors Govern Liquidlike Ordering and Fusion Dynamics of Bacterial Colonies, *Phys. Rev. Lett.*, **121**:118102 (2018).

[12] Li Y., Perera L., Coons L.A., Burns K.A., Tyler Ramsey J., Pelch K.E., Houtman R., van Beuningen R., Teng C.T., Korach K.S., Differential in Vitro Biological Action, Coregulator Interactions, and Molecular Dynamic Analysis of Bisphenol A (BPA), BPAF, and BPS Ligand–ER α Complexes, *Environ. Health Perspect*, **126**:17012 (2018).

[13] Liu J., Zhu H., Wang H., Li J., Han F., Liu Y., Zhang W., He T., Li N., Zheng Z., Hu D., Methylation of Secreted Frizzled-Related Protein 1 (SFRP1) Promoter Downregulates Wnt/β-Catenin Activity in Keloids, *J. Mol. Histol.*, **49**: 185–193 (2018).

[14] Lin Y., van Duyvenvoorde H.A., Liu H., Yang C., Warsito D., Yin C., Kant S.G., Haglund F., Wit J.M., Larsson O., Characterization of an Activating R1353H Insulin-Like Growth Factor 1 Receptor Variant in a Male with Extreme Tall Height, *Eur. J. Endocrinol.*, **179**: 85–95 (2018).

[15] Zhao Y., Ding C-H., In vitro Effects of Nerve Growth Factor on Cardiac Fibroblasts Proliferation, Cell Cycle, Migration, and Myofibroblast Transformation, *Chin. Med. J. (Eng.)*, **131**:813 (2018).

[16] Campos M., Govers S.K., Irnov I., Dobihal G.S., Cornet F., Jacobs- Wagner C., Genomewide Phenotypic Analysis of Growth, Cell Morphogenesis, and Cell Cycle Events in Escherichia Coli, *Mol. Syst. Biol.*, **14**: e7573 (2018).

[17] Iverson P., Song J., Bradley H., Cortical Entrainment to Speech Under Competing-Talker Conditions: Effects of Cognitive Load Due to Presentation Rate and Task Difficulty, *J. Acoust. Soc. Am.,* **143**:1921 (2018).

Research Article